# Analyzing PSDM images in complex geology via ray-based PSF-convolution modeling

*Kristian Jensen* and Isabelle Lecomte, University of Bergen; Tina Kaschwich, NORSAR*

**Summary**

A common problem encountered when migrating seismic data is the blurring and partial retrieval of the stratigraphic model of interest due to limited survey illumination, propagation effect functions of the overburden velocity, frequency-band limited wavelets, and more. Through the application of ray-generated 2(3)D spatial convolution operators, referred to as *point-spread functions (PSFs)*, these blurring effects and partial illumination may be analyzed in more detail, which enhances our understanding of seismic image quality, prior or after acquisition and processing. To illustrate our purpose, we apply the method on the synthetic Sigsbee2A model at selected target areas, and study how, e.g., amplitude effects and aperture width affect the migrated image. A ray approach allows indeed for efficient sensitivity studies on various parameters, thus explaining differences in seismic image quality, while possibly helping fine-tuning imaging parameters.

**Introduction**

Seismic imaging often yields a blurred and partial version of the elastic parameters of interest due to limited survey illumination, complex velocity models, and wavelet effects. These limited-illumination and resolution effects may in some cases be severe enough to completely mask or distort geological features of interest, even if the velocity model used for the migration is correct, and therefore have to be accounted for to allow a proper interpretation.

As outlined in Lecomte (2008), the application of 2(3)D spatial convolution operators, referred to as *point-spread functions* (PSFs) generated by ray-based information, may be used to simulate prestack depth migrated (PSDM) images at a cost similar to 1D-convolution. The PSFs represent the local-target Hessian operators of a migration, and, when plotted in the wavenumber domain, enable us to obtain an intuitive understanding of the quality of the migrated image around a local target-point (Gelius *et al*., 2002).

In the present work, we apply the ray-based method on the synthetic 2D acoustic Sigsbee2A model, which consists of a complex fault-dominated stratigraphy of sedimentary blocks incorporating a large salt body (Paffenholz *et al*., 2002). The use of PSFs for studying illumination properties of the Sigsbee2A model has been well documented in recent studies such as Tang (2009), Thomson *et al*. (2016), and Lecerf and Besselievre (2018). The application of a ray-based PSF-convolution method on that model for studying limited-illumination and resolution effects allows additional insights into seismic imaging issues in complex geology. We illustrate here how the method may assist in better understanding the migration process and the quality of the resulting seismic images. In particular, and for the sake of illustration, we explore how migration aperture and failing to compensate for amplitude effects in the migration process may distort seismic images to such an extent that important geological features are not imaged.

**Theory: ray-based PSF-convolution modeling**

Ray tracing is used to estimate the PSF by calculating the slowness vectors attached to the incident and scattered wavefields ($\boldsymbol{p_s}$ and $\boldsymbol{p_r}$) at a chosen image point for all shot-receiver pairs in a survey. So-called illumination vectors, $\boldsymbol{l_{SR}}$, at the point may then be calculated as $\boldsymbol{l_{SR} = p_R - p_S}$. The orientation of an $\boldsymbol{l_{SR}}$ depends on the incident and scattered directions, and the length of the vector depends on medium velocity and opening angle between $\boldsymbol{p_s}$ and $\boldsymbol{p_r}$ (Lecomte, 2008). The fan of $\boldsymbol{l_{SR}}$ at the point will illustrate the local dip range of reflectors which may be imaged, also constraining the along-reflector resolution, whereas the lengths determines the across-reflector resolution. By multiplying the $\boldsymbol{l_{SR}}$ with frequency, we obtain the *scattering wavenumber vectors* at the point, thus obtaining the PSDM filter in the wavenumber domain. A Fourier Transform will then yield the PSF in the space domain (PSDM image of a point scatterer). **Figure 1** illustrates the latter part of this procedure in the 2D case. The PSF may then be convolved with an input reflectivity grid to generate a (simulated) PSDM seismic image (Lecomte et al., 2003).

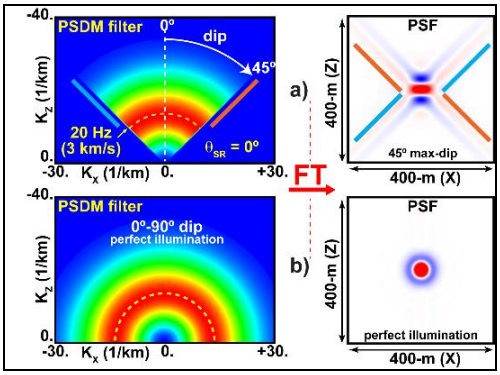


**Figure 1 (a-left):** PSDM filter with velocity 3 km/s, zero-offset acquisition, 20-Hz Ricker, and dip range between -45° and +45°. **(a-right):** Fourier Transform of (a-left). **(b-left):** PSDM filter with dip range changed to -90° and +90° (perfect illumination). **(b-right):** Fourier Transform of (b-left). Image obtained from Lecomte *et al*. (2016).



10.1190/segam2018-2995975.1

Although the abovementioned method for calculating PSFs is ray-based, full-waveform generated PSFs may also be used (e.g., Tang, 2009; Toxopeus *et al.*, 2010). The latter approach comes however at higher computational cost and with less flexibility for interactive sensitivity analyses (Lecomte *et al.*, 2016), which is illustrated here. Both approaches are complementary in practice.

**Ray-based PSF-convolution modeling on Sigsbee2A**

The ray-based PSF-convolution method was applied on two selected target areas of the Sigsbee2A model dominated by transverse faults (*Target A*, and *Target B*; **Figure 2**). A PSF was generated at the center of each target. The 2D seismic survey corresponding to the initial marine acquisition parameters for the Sgisbee2A model was considered, and a zero-phase Ricker wavelet with peak frequency of 20 Hz was used as pulse. Turning waves were not included.

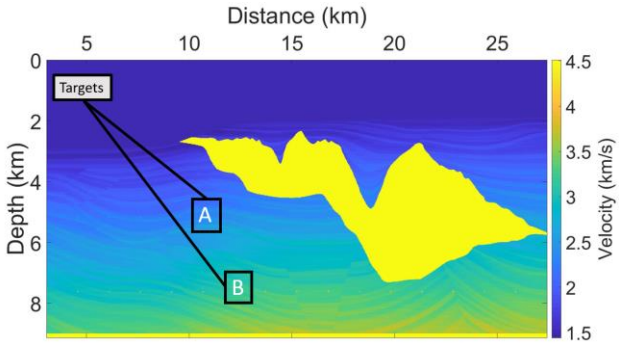


**Figure 2:** the Sigsbee2A stratigraphic velocity model with the selected target areas (A and B). A PSF was generated at the center of each target and used to simulate local PSDM images.

The reflectivity grids of the two target areas are illustrated in **Figure 3**. PSDM images obtained by Tang (2009) on the same target areas through PSFs generated by a phase-encoded Hessian operator using one-way wave-equation based Fourier finite-difference (FFD) migration (Ristow and Rühl, 1994) are included in **Figure 4.** These images illustrate well the difficulties in obtaining proper imaging of the transverse faults, in particular at Target B, due to poor illumination of the targets, as will now be illustrated by a ray analysis. To illustrate the effects of various migration parameters - and versatility of a ray approach – PSDM images at 8-km and 2-km aperture widths, respectively, were generated in "true amplitude" mode ($I_{SR}$ equally weighted). Similar images were generated for raw (uncorrected) amplitudes for both aperture widths. The same relative scaling of amplitudes was done for visual comparison. The corresponding zero-offset raypaths are illustrated in **Figure 5** for the sake of illustration.

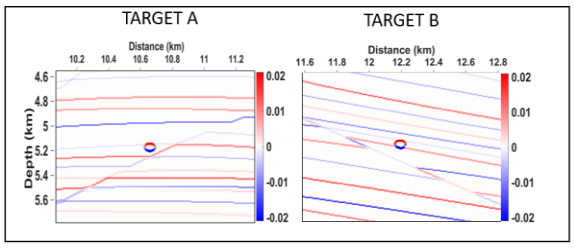


**Figure 3 (left):** input reflectivity for Target A. **(right):** input reflectivity for Target B.

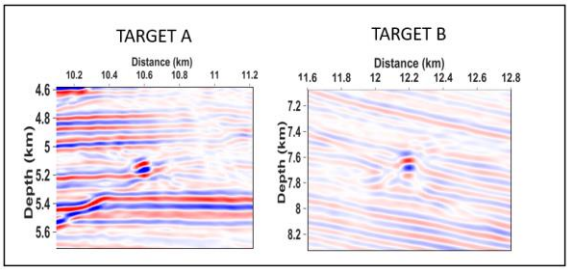


**Figure 4 (left):** Target A generated by Tang (2009). **(right):** Target B generated by Tang (2009). Amplitudes are scaled relatively for comparison purposes.

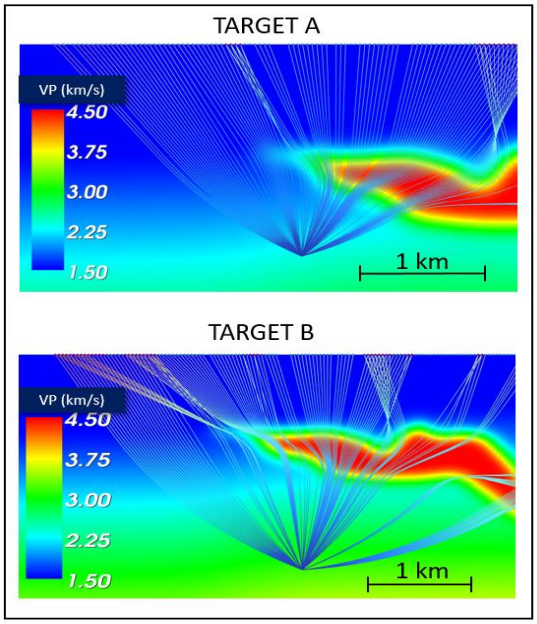


**Figure 5 (upper):** zero-offset raypaths to Target A. **(lower):** zero-offset raypaths to Target B. (1x1 aspect ratio).

DOI:10.1190/segam2018-2995975.1

The seismic images obtained when convolving the reflectivity grids with target-oriented PSFs are illustrated in **Figure 6** (Target A) and **Figure 7** (Target B). As can been seen in **Figure 6**, Target A is well-illuminated (wide range of dip angles, cf. **Figure 5**), meaning that all dips within the input reflectivity are captured when true amplitude is preserved, and a wide aperture width of 8 km is applied. A smaller 2-km aperture width will, however, limit the dip range possible at the target point, and, as a result, the transverse fault is blurred. When raw, uncorrected, amplitudes are considered, the fault is still imaged at 8-km wide aperture width, but the seismic waves that have passed through the salt body will have suffered a strong loss of energy due to geometrical spreading and lack of compensation for this. This is illustrated well in the corresponding PSDM filter. However, as the transverse fault is perpendicular to the well-illuminated part of the target, it still remains visible, although the seismic image in general becomes more blurred as having a slightly lower illumination results in a worse lateral resolution. Finally, the seismic image obtained for raw, uncorrected amplitudes at a 2 km wide aperture width fails to illuminate the fault due to the same limited dip range as for the true amplitude case, while also suffering blurring effects due to limited lateral resolution.

**Figure 7** illustrates many of the same effects for Target B, but the imaging challenges are even more prominent here. For true amplitude, 8-km wide aperture width, the transverse fault is illuminated, although poor lateral resolution is evident, resulting from loss of high-frequency energy due to the depth of the target. At a 2-km wide aperture width, the fault is not imaged because the dip of the fault falls outside the possible dip range obtained. When raw amplitudes are considered, the dip range becomes severely limited as the loss of energy due to geometrical spreading in the salt body is even more evident than for Target A. It is no longer possibly to image the fault, and the lack of proper lateral resolution is also now clearly evident in the smearing of the obtained PSF. As a result, artefacts occur in the obtained seismic image due to lack of constructive interference of the scattering migration isochrones. The same issues are also valid for the image generated through raw amplitudes, 2-km wide aperture width, although the smearing effect this time occurs in a slightly different direction due to the lack of illumination at wider angles.

## Conclusions

We illustrate how ray-based Point-Spread Functions (PSFs) used as versatile spatial convolution operators may be applied to model limited illumination and blurring effects commonly observed in migrated seismic data. By applying the method on two selected target areas in the Sigsbee2A model, we show how such a modeling may be useful to investigate how target areas in complex geological settings may yield different quality of migrated seismic images due to, e.g., amplitude effects and varying aperture widths. Ray-generated PSFs may therefore, as an alternative or complement to computationally costly wave-equation based methods, offer an efficient and flexible method for simulating partial illumination and blurring effects in complex models, adding some of the imaging parameters in the analyses. In the specific case of Sigsbee2A and other benchmark models, it is however highly necessary to have full control on all input parameters (modeling and imaging), for more thorough and quantitative studies allowing for a direct comparison with wave-equation generated PSFs. and such a study is ongoing for Sigsbee2A and other data sets.

## Acknowledgments

The first author wishes to thank the University of Bergen for PhD-project funding. All authors thank and acknowledge Dr. Yaxun Tang for providing datasets used in Tang (2009) as well as the SMAART JV consortium for providing the Sigsbee2A dataset. Further, all authors wish to thank NORSAR Innovation AS for the use of their modeling software. Lastly, the authors thank the Research Council of Norway for some financial support through project #267634/E30 (FOPAK) and Uni Research, project owner.

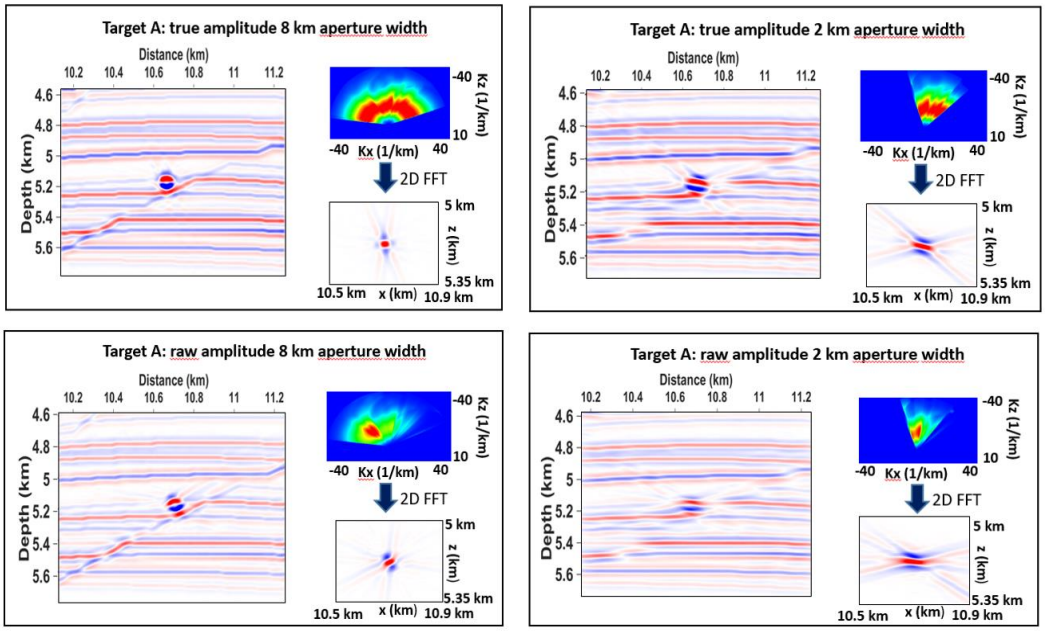


**Figure 6:** Illumination of Target A depending on true versus raw amplitude, and aperture width. Each subfigure includes generated seismic data, corresponding PSDM filter and corresponding PSF generated in the x-z domain. Amplitudes are scaled relatively for comparison purposes.

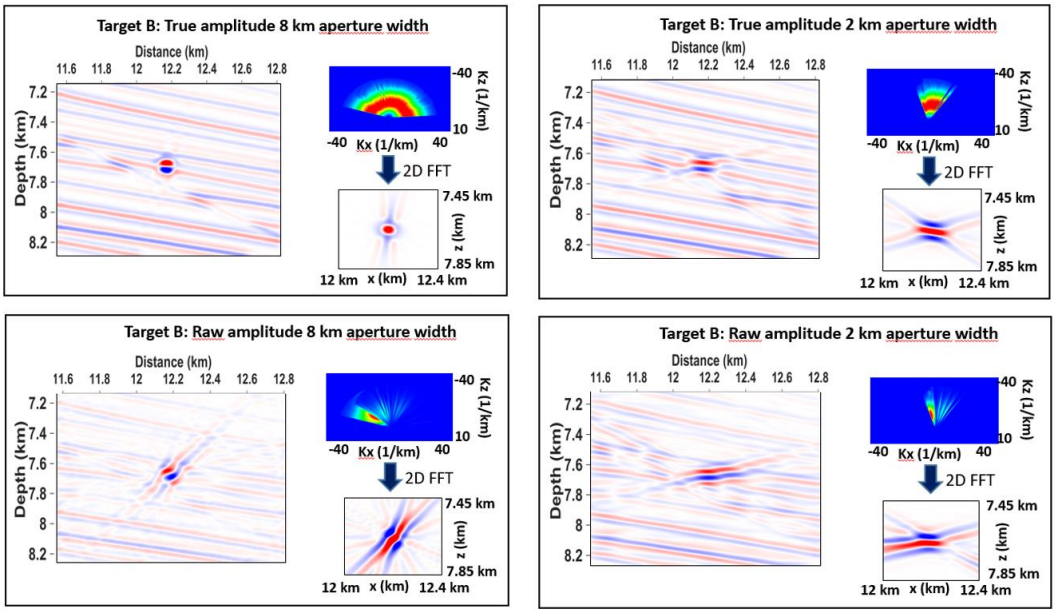


**Figure 7:** Illumination of Target B depending on true versus raw amplitude, and aperture width. Each subfigure includes generated seismic data, corresponding PSDM filter and corresponding PSF generated in the x-z domain. Amplitudes are scaled relatively for comparison purposes.



10.1190/segam2018-2995975.1

## REFERENCES


Gelius, L.-J., I. Lecomte, and H. Tabti, 2002, Analysis of the resolution function in seismic prestack depth imaging: Geophysical Prospecting, **50**, 505–515, https://doi.org/10.1046/j.1365-2478.2002.00331.x.

Lecerf, D., and M. Besselievre, 2018, A new approach to compensate for illumination differences in 4D surveys with different individual acquisition geometries: First Break, **36**, 71–76.

Lecomte, I., 2008, Resolution and illumination analyses in PSDM: A ray-based approach: The Leading Edge, **27**, 650–663, https://doi.org/10.1190/1.2919584.

Lecomte, I., and H. Gjøystdal, and Å. Drottning, 2003, Simulated prestack local imaging: A robust and efficient interpretation tool to control illumination, resolution, and time-lapse properties of reservoirs: 73rd Annual International Meeting, SEG, Expanded Abstracts, 1525–1528, https://doi.org/10.1190/1.1817585.

Lecomte, I., P. Lubrano Lavadera, C. Botter, I. Anell, S. J. Buckley, C. H. Eide, A. Grippa, V. Mascolo, and S. Kjoberg, 2016, 2(3)-D convolution modelling of complex geological targets—Beyond 1D convolution: First Break, **34**, 99–107.

Paffenholz, J., J. Stefani, B. McLain, and K. Bishop, 2002, SIGSBEE_2A synthetic subsalt dataset—Image quality as function of migration algorithm and velocity model error: 64th Annual International Conference and Exhibition, EAGE, Extended Abstracts, B019.

Ristow, D., and T. Rühl, 1994, Fourier finite-difference migration: Geophysics, **59**, 1882–1893, https://doi.org/10.1190/1.1443575.

Tang, Y., 2009, Target-oriented wave-equation least-squares migration/inversion with phase-encoded Hessian: Geophysics, **74**, no. 6, WCA95–WCA107, https://doi.org/10.1190/1.3204768.

Thomson, C. J., P. W. Kitchenside, and R. P. Fletcher, 2016, Theory of reflectivity blurring in seismic depth imaging: Geophysical Journal International, **205**, 837–855, https://doi.org/10.1093/gji/ggw025.

Toxopeus, G., and J. Thorbecke, 2010, A brief summary of Hessian based modelling in a shared earth environment: 72nd Annual International Conference and Exhibition, EAGE, Extended Abstracts, https://doi.org/10.3997/2214-4609.201401319.